Chemical Papers
https://doi.org/10.1007/s11696-026-05240-3

ORIGINAL PAPER

Electrochemical analysis of tetracycline in drug formulations with glutardialdehyde-Fe_2O_3 modified glassy carbon electrode

Berna Koçak[1] · **Yeliz İpek**[1]

Received: 4 March 2026 / Accepted: 19 June 2026
© The Author(s) 2026

Abstract

In this study, a glutardialdehyde-Fe_2O_3 modified glassy carbon electrode (GA_2–Fe_2O_3/GCE) was used as a sensor for the electrochemical analysis of tetracycline (TC) in drug formulations. The electrochemical behavior of TC on GA_2-Fe_2O_3/GCE was investigated using cyclic voltammetry (CV), while the quantitative determination was performed via differential pulse voltammetry (DPV). After optimizing the experimental conditions, the linear working range, limit of (LOD) detection, and limit of quantification (LOQ) of the GA_2-Fe_2O_3/GCE electrode developed for the electrochemical analysis of TC were found to be 1.0×10^{-6}–2.0×10^{-5} M and 2.0×10^{-5}–9.9×10^{-6} M; 4.78×10^{-7} M; 1.59×10^{-6} M, respectively. In the sensor application study conducted on a Tetra® Gensenta tablet to demonstrate the applicability of the developed method, the linear working range, LOD, and LOQ values of the sensor were found to be 1.0×10^{-6}–14.8×10^{-5} M; 5.72×10^{-7} M and 1.74×10^{-6} M, respectively. The applicability of the method was demonstrated through tablet recovery studies, and the tablet recovery ratio was determined to be 100.94%.

Graphical abstract

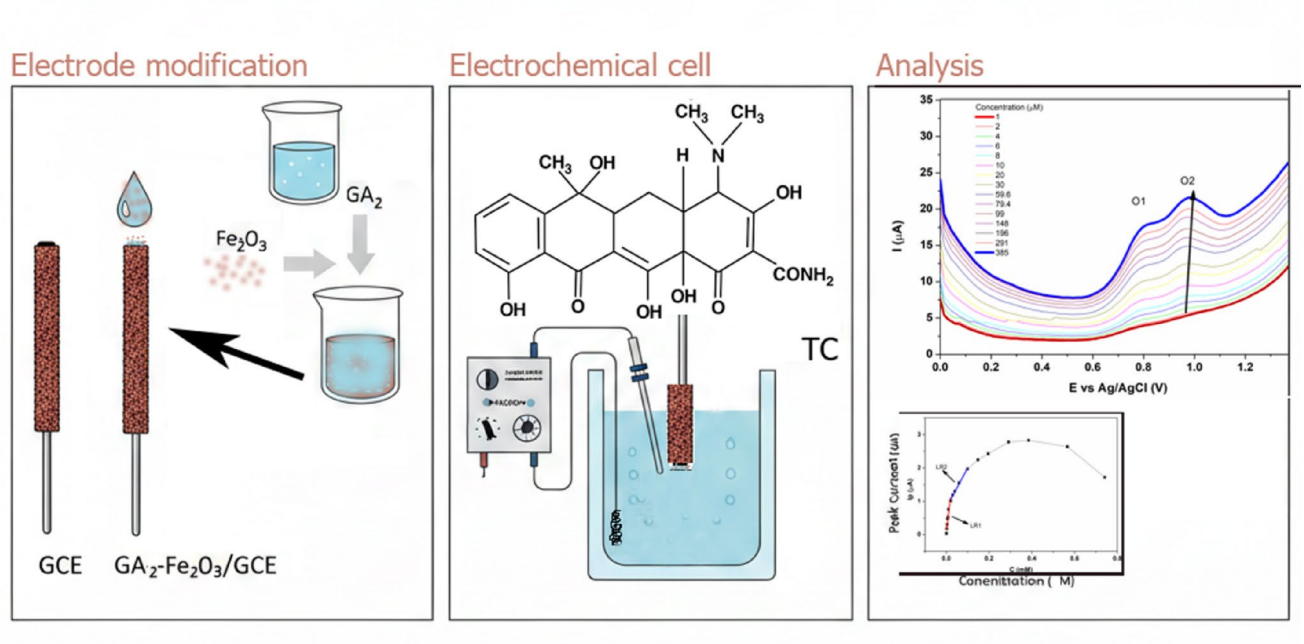

Keywords Tetracycline · Fe_2O_3 · Glutardialdehyde · Electrochemical analysis · Voltammetry · Modified electrode

Extended author information available on the last page of the article

Published online: 02 July 2026

Introduction

Tetracyclines (TCs) (including tetracycline (TC), oxytetracycline (OTC), chlortetracycline (CTC), and doxycycline (DOC)) are broad-spectrum antibiotics used to treat bacterial infections and promote agricultural growth, first discovered in 1940. Tetracycline is effective against both gram-negative and gram-positive bacteria (Luo et al. 2025, ; Wang et al. 2024; Zhang et al. 2024a, b). The TC molecular structure is shown in Fig. S1.

Additionally, tetracycline can be used to inhibit the growth of atypical organisms such as Mycoplasma, Chlamydia, and Rickettsia, as well as protozoan parasites (Zhao et al. 2024).

Tetracyclines (TCs) are widely used in livestock farming (as feed additives), aquaculture, and the treatment of animal diseases due to their antibacterial properties and robust therapeutic effects. One of the main reasons for this is their strong bacterial inhibition and low cost(Chang et al. 2023). Excessive and indiscriminate use of tetracyclines pollutes soil and groundwater. This causes serious harm to both human health and the environment (Zhang et al. 2024a, b; Hu et al. 2024; Chen et al. 2024).

TC residues found in animal foods cause antibiotic resistance and may prolong treatment time. In addition, TC residues found in groundwater and soil can be a threat to biodiversity in the ecosystem (Chen et al. 2024; Zhao et al. 2024; Zhang et al. 2024a, b).

Therefore, it is important to develop sensitive and accurate analytical methods for the use of tetracyclines, the detection of residue levels, and the reduction of their environmental impacts. Various studies have been conducted on the determination of TC. Analysis was performed using HPLC (Adabi et al. 2024; Butovskaya et al. 2024; Taşcı et al. 2021; Gab-Allah et al. 2023; Meklati et al. 2022), colorimetry (Urapen and Masawat 2015; Zhao et al. 2024), enzyme-linked immunosorbent assay (ELISA) (Wang et al. 2021), fluorescence method (Zhou et al. 2018), and electrochemical methods (Guo et al. 2024; Zhang et al. 2024a, b; Wang et al. 2024; Sun et al. 2025; Nekoueian et al. 2024; Gao et al. 2024). The following section has been added to the text. However, these techniques are limited due to high solvent consumption, the need for expensive equipment, the necessity of a specialized laboratory environment, and the need for highly trained personnel (Koçak 2023; Metto et al. 2024, 2025). In this study, the electrochemical method was preferred for the analysis of TC because electrochemical methods are fast, selective, and sensitive analytical methods that do not require any prior separation (Koçak 2023). In electrochemical studies, glutaraldehyde (GA) or glutardialdehyde (GA_f) has been used as a binder to immobilize the substance that can interact with the analyte and is used in the modification of the electrode surface (İpek 2020; Koçak et al. 2023; Koçak and İpek 2022; Keçeçi et al. 2025).

Metal oxide nanoparticles are used in electrochemical sensors due to their structural, electronic, and surface properties (Sato et al. 2023). Hematite Fe_2O_3 (n-type metal oxide), in particular, has recently become a focus of attention due to its narrow band gap (Eg = 2.2 eV), low cost, ease of production and storage, and non-toxicity (; Iqbal et al. 2025; Gupta et al. 2026). Fe_2O_3 nanoparticles have been preferred in many industrial processes (electronic and optical devices, data storage, color imaging, bioprocessing, ferrofluid technology, and production of magnetic recording media) due to their electronic, magnetic, and optical properties (Vinay and Nayaka 2019). Numerous studies exist using electrodes modified with Fe_2O_3 nanoparticles (Sato et al. 2023; Abood et al. 2021; Harraz et al. 2016; Vinay et al. 2019).

In this study, a glassy carbon electrode modified with GA_2-Fe_2O_3 was used. The electrode surface was modified using a simple drop-in method. The behavior of tetracycline on the electrode surface was determined using cyclic voltammetry (CV), and quantitative analysis on the electrode surface was performed using differential pulse voltammetry (DPV). The accuracy of the method was verified through tablet recovery studies.

Experimental

Instrumentation

In electrochemical studies, an Ivium pocketstat (potentialiostat galvanostat impedance analyzer) was used, pH measurements were performed using an Ohaus starter 3000 Bench pH meter, weighing was done using a Bell brand balance (with ± 0.0001 g accuracy), and ultra-pure water was obtained using a millipore direct- 3QV brand device in experimental studies.

Electrodes

In electrochemical studies, GCE, GA_2-Fe_2O_3/GCE were used as working electrodes, Ag/AgCl (3 M NaCl) electrode (MF-2052, BASİ) was used as a reference electrode, and Pt wire was used as a counter electrode.

Reagents and chemicals

TC (pure form) was obtained from Sigma Tetra® Gensenta tablets were obtained from a pharmacy. All chemicals used were of analytical grade; glutardialdehyde used in electrode surface modification was obtained from Merck, and Fe_2O_3 from Merck. Company. Sodium hydroxide (NaOH), acetic

acid (CH_3COOH), and phosphoric acid (H_3PO_4) used in the preparation of the buffer solution were obtained from Sigma Aldrich. Boric acid (H_3BO_3) was obtained from Fisher Chemical Company.

Cleaning the GCE surface and preparing the modified electrode

To obtain reproducible results with GCE, which was used as the working electrode in experimental studies, a small amount of aluminum oxide (alumina, Al_2O_3, 0.05 µm) was poured onto the polishing pad before each experimental study and before modifying the electrode surface. The pad was then cleaned by making figure-eight movements on the slurry with deionized water, and subsequently rinsed with deionized water. The surface of the polished GCE was modified via the drop-casting method. To prepare the modified electrode (GA_2-GCE), 5 µL of a 5% glutaraldehyde solution (GA_2) was applied onto the GCE surface and allowed to dry under ambient conditions. Similarly, Fe_2O_3-GA_2/GCE modified electrodes were fabricated separately by drop-casting 5 µL of their respective metal oxide-GA_2 solutions (1 mg/mL concentration) onto the GCE surfaces, followed by drying at room temperature. During the preparation of these modified electrodes, the concentrations of GA_2 and metal oxide were determined based on existing literature. Observations indicated that metal oxide amounts below 1 mg coated the GA_2 surface and led to a decrease in peak current, whereas excessive amounts resulted in the flaking of the electrode surface coating (Koçak 2023; Koçak and İpek 2022).

Preparation of solutions

The TC stock solution was prepared in ethanol. 0.245 g of TC was weighed, and the volume was completed to 50 mL in a volumetric flask. The resulting gentamicin sulfate solution, with a concentration of 1.0×10^{-2} M, was stored in a refrigerator at + 4 °C in a dark environment. Dilution processes were performed by taking samples from this solution.

Britton-Robinson (BR) buffer was preferred as the supporting electrolyte medium. To prepare this buffer solution, 2.69 mL of phosphoric acid (99.5% purity), 2.29 mL of acetic acid (99.8–100.5% purity), and 2.472 g of boric acid (99.5% purity) were mixed, and the volume was completed to 1 L with deionized water. The buffer solution was prepared at the desired pH by adding 0.1 M HCl or 0.1 M NaOH to the prepared solution. Preparation of 0.1 M NaOH solution 1.000 g of sodium hydroxide (NaOH) was dissolved in a quantity of ultra-pure water in a 250 mL volumetric flask, and the volume was then completed to 250 mL with ultra-pure water. Preparation of 0.1 M HCl Solution 1.33 mL of concentrated hydrochloric acid (with a density of 1.86 g mL^{-1} and 37% (m/m) concentration) was taken, and the volume was completed to 250 mL with ultra-pure water in a 250 mL volumetric flask.

Results and discussion

Electrochemical characterization of GA_2-Fe_2O_3/GCE

Surface characterizations of GCE and GA_2-Fe_2O_3/GCE were performed by CV and EIS methods. In order to determine the difference between the GCE surface and the GA_2-Fe_2O_3/GCE surface, CV voltammograms were measured and recorded in 1 mmol L^{-1} $K_3Fe(CN)_6$ and 0.1 mol L^{-1} KCl solution. These voltammograms are shown in Fig. S2.

Table 1 shows the anodic and cathodic peak current values and peak potential values of cyclic voltammograms taken in GCE and GA_2-Fe_2O_3/GCE and 1 mmol L^{-1} $K_3Fe(CN)_6$ and 0.1 mol L^{-1} KCl solution.

As seen in Table 1, while the peak potential difference (ΔE) for GCE was 0.3 V, the peak potential difference for GA_2-Fe_2O_3/GCE increased to 0.7 V and the anodic peak current values also decreased. Additionally, the fact that the Ipk/Ipa value of GA_2-Fe_2O_3/GCE is equal to 0.98 indicates that the reversibility and electron transfer rate at this electrode surface are close to that of GCE.

Electrochemical characterizations performed on electrodes are intended to show whether modifications made to the electrode affect the electroactive surface area of the electrode surface (Koçak et al. 2023). Therefore, to show whether there is a change in the surface area of the GCE electrode modified with GA_2-Fe_2O_3, cyclic voltammograms were obtained on GCE and GA_2-Fe_2O_3/GCE at different scan rates (5–1000 mV s^{-1}) in 1 mM $K_3Fe(CN)_6$ and 0.1 M KCl solutions as a probe redox system at different temperatures. These voltammograms are shown in Fig. 1.

The slope of the graph $v^{1/2}$—Ip plotted (Fig. 2) using these voltamograms was used in the Randles–Sevcik equation, which is the area determination equation (Bard et al., 2022; Dinber et al. 2024). The equation is given below.

Table 1 Anodic and cathodic peak current values and peak potential values of voltammograms recorded with GCE and GA_2-Fe_2O_3/GCE electrodes in 1 mmol L^{-1} $K_3Fe(CN)_6$ and 0.1 mol L^{-1} KCl solution

	Anodic		Cathodic			
	Ip_a(µA)	E(V)	Ip_k(µA)	E(V)	Ip_k/Ip_a	ΔE(V)
GCE	6.96	0.310	−7.26	0.22	1.04	0.3
GA_2-Fe_2O_3/GCE	4.30	0.370	−4.37	0.175	0.98	0.7

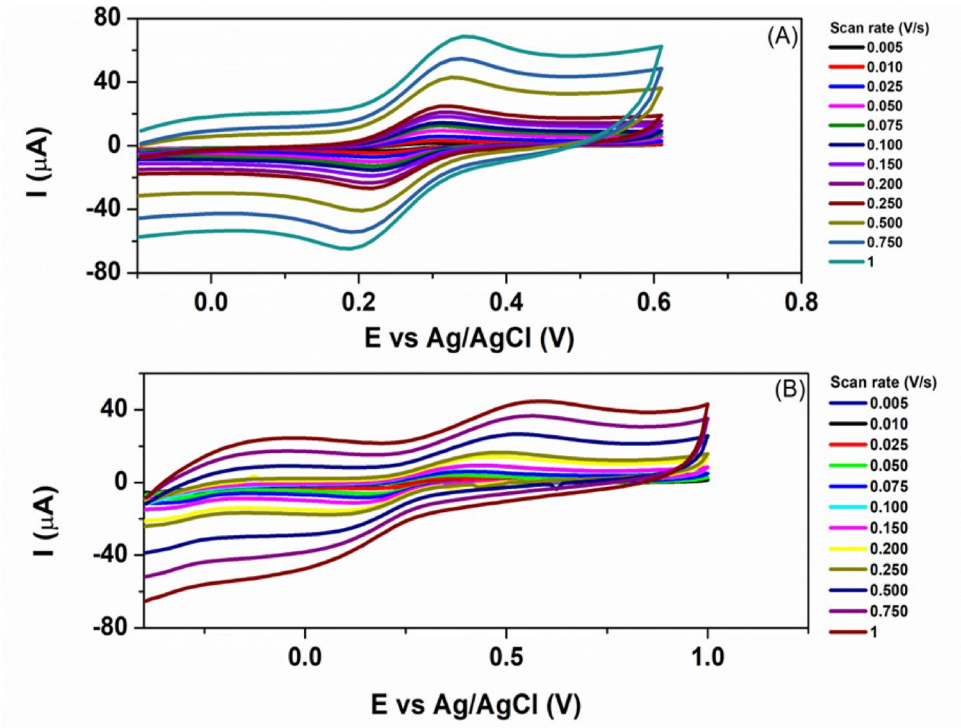

Fig. 1 Voltamograms obtained with **A** GCE and **B** GA_2-Fe_2O_3/GCE in 1 mM $K_3Fe(CN)_6$ and 0.1 M KCl solution in the scan rate range of 5–1000 mV/s

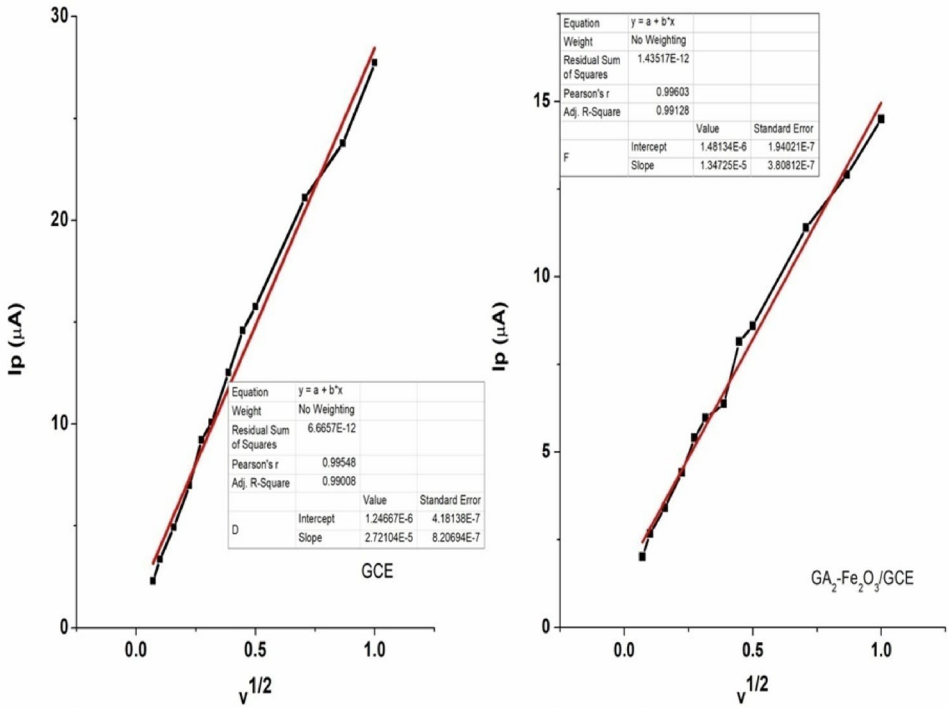

Fig. 2 $v^{1/2}$-Ip graphs of GCE and GA_2-Fe_2O_3/GCE in 1 mM $K_3Fe(CN)_6$ and 0.1 M KCl solution in the scan rate range of 5–1000 mV s^{-1}

$$I_p = 2.69\text{x}10^5 ACn^{3/2}D^{1/2}v^{1/2}$$

In the equation, Ip: Oxidation peak current (A), A: Electroactive surface area of the electrode (cm^2), C: Molar concentration of $K_3Fe(CN)_6$ solution, n: Number of electrons transferred in the redox reaction, and D: Diffusion coefficient of $K_3Fe(CN)_6$ ($cm^2\ s^{-1}$), v: Scanning rate ($V{\bullet}s^{-1}$) (n = 1, D = 7.6×10^{-6} $cm^2\ s^{-1}$ and C = 1.0×10^{-6} mmol•cm^{-3} represents the concentration of $K_3Fe(CN)_6$ in 0.1 mol•L^{-1}KCl electrolyte. Prior to the modification, the geometric surface area of the GCE was 0.071 cm^2. The surface areas of GCE and GA_2-Fe_2O_3/GCE were calculated according to Randles–Sevcik and are 0.0196 cm^2 and 0.0098 cm^2, respectively. Although the electroactive surface area of GA_2-Fe_2O_3/GCE

Table 2 The peak currents of TC on the GCE and GA_2-Fe_2O_3/GCE electrodes

Technique	Electrode	E_1(V)	Ip_1(A)	E_2(V)	Ip_2(A)
CV	GCE	0.770	1.19×10^{-7}	0.96	1.175×10^{-7}
	GA_2-Fe_2O_3/GCE	0.800	6.78×10^{-8}	0.99	8.11×10^{-8}
DPV	GCE	0.70	1.64×10^{-6}	0.88	9.44×10^{-7}
	GA_2-Fe_2O_3/GCE	0.75	5.35×10^{-7}	0.97	1.09×10^{-6}

is lower than that of GCE. In the analysis of the TC with the modified electrode, the peak current of the modified electrode was found to be higher. These results are shown in Table 1. Although the surface area of the Fe_2O_3-GA_2/GCE is smaller than the GCE surface area, Table 2 shows that the modified electrode has a more selective effect compared to TC.

Surface characterization of GCE, GA_2/GCE, Fe_2O_3-GA_2/GCE was performed using the EIS method. EIS analysis was applied in the 100–0.1 Hz range, and a C′ vs C″ graph was plotted (Fig. S3). This graph allows you to see more clearly how much ion transfer is allowed by the porous structure of the electrode and the power density of the system. A semicircle was formed here, and the increase in the diameter of the circle indicates that the total storage capacity (C′) of the system has increased. The diameter of the circle widened after modification with GA_2, and a slight narrowing occurred when Fe_2O_3 was added to the structure. The widening and spreading of the circle diameter indicates an increase in surface roughness or porosity (Magar et al 2021).

SEM–EDS characterization of GA_2-Fe_2O_3/GCE

The presence of Fe in the GA_2-Fe_2O_3 structure was investigated using EDS, and the morphology of the thin film on the electrode was examined using SEM. Fig. S4 is the SEM–EDS image of GA_2, and Fig. 3 is the SEM–EDS image of GA_2-Fe_2O_3. SEM was used to show the high-resolution morphological structure of the substances modified on the electrode surface. An examination of the glass surfaces modified with GA_2 and GA_2-Fe_2O_3 reveals that the latter exhibits a more pronounced surface roughness, as illustrated in Fig. S4. This increased roughness facilitates charge transfer, thereby enhancing the sensitivity of the electrode (Burç et al. 2024).

Investigation of the behavior of tetracycline on GA_2-Fe_2O_3/GCE

The electrochemical behavior of TC was investigated using the CV method on GCE and GA_2-Fe_2O_3/GCE. The voltammetric behavior of TC was investigated at pH 6.0 with bare GCE and GA_2-Fe_2O_3/GCE using the CV and DPV methods between 0–1.5 V. Two irreversible oxidation peaks were observed for tetracycline. Their peak potentials and peak currents are given in Table 2. Tetracycline characteristically possesses various functional groups, including phenolic and di(methyl)amino substituents. Electrochemical oxidation is thought to occur through these groups (Cánovas et al 2021).

Table 2 shows the peak potentials and currents of voltamograms recorded using bare GCE and GA_2-Fe_2O_3/

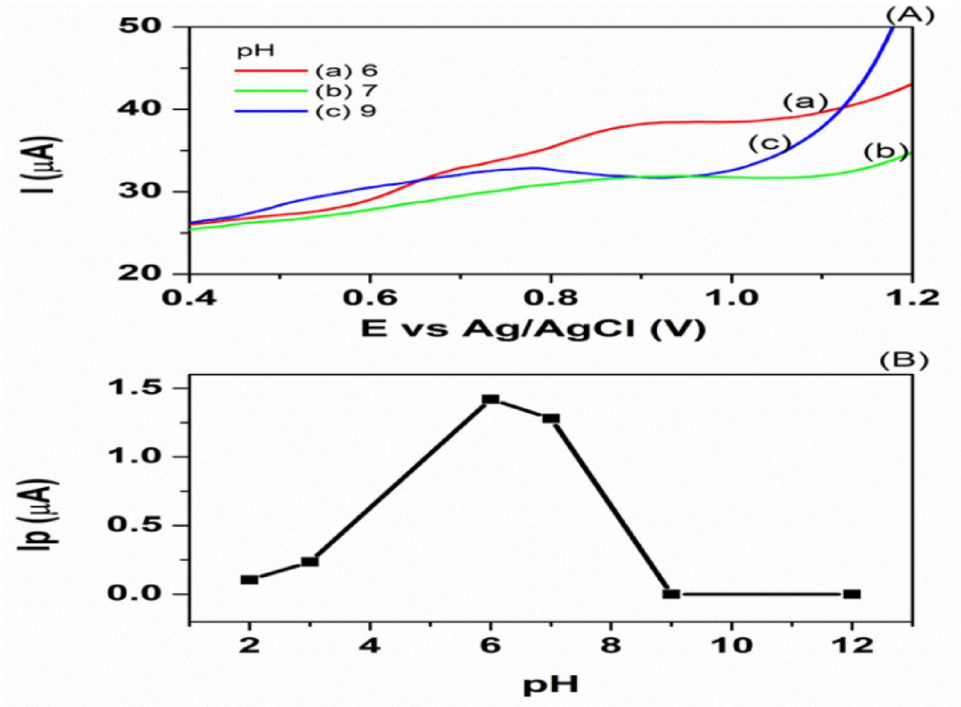

Fig. 3 **A** DPV voltamograms recorded in BR buffer at different pH levels of 2.99×10^{-5} M TC, **B** pH-Ip graph

GCE working electrodes with 2.99×10^{-5} M TC (scan rate 50 mV s^{-1}). Initially, voltamograms were obtained with GCE and then with GA_2-Fe_2O_3/GCE in pH 6 Britton Robinson (BR) buffer solution(Fig. S5). When TC was added to 10 mL of pH 6 buffer at a concentration of 2.99×10^{-5} M, the current values of the second peak in the obtained voltamograms were compared, and it was observed that the current was 9.44×10^{-7}A with the GCE electrode and 1.09×10^{-6}A with the GA_2-Fe_2O_3/GCE electrode. A slight shift in peak potentials was observed due to the use of GA_2 in the modification process. It is thought that Fe_2O_3 supports the amplification of the second peak and therefore the peak current is increased. In subsequent studies, the GA_2-Fe_2O_3/GCE electrode, which has a good electrocatalytic effect and sensitivity against TC, was used (Koçak 2023; Koçak et al.2023).

Determination of optimum pH

To investigate the effect of pH on the electrochemical behavior of tetracycline, BR buffer was chosen. This is because the Britton-Robinson (B-R) buffer solution is preferred as a supporting electrolyte due to its broad buffering capacity between pH 2 and 12. In addition, there are literature studies indicating that "BR" buffer is preferred in electrochemical studies of tetracycline (Allahverdiyeva et al 2021; Gholivand et al. 2013; Đurović et al 2022). The change in peak current of a solution containing tetracycline at a concentration of 2.99×10^{-5} M was investigated in BR buffer at pH 3.0–12.0 using the DPV method. Two peaks were observed in the acidic region (pH 3–6), and at pH 7–9, the peaks merged to form a broad peak. At pH 12, no oxidation peak was observed. At pH 3, the 1st and 2nd peak potentials and 1st and 2nd peak currents of TC were as follows: 0.89;1.072 V and 6.04×10^{-7};2.69×10^{-7} A, respectively. At pH 6, the 1st and 2nd peak potentials and 1st and 2nd peak currents of TC were as follows: 0.67; 0.88 V and 4.23×10^{-7};1.42×10^{-6} A. TC possesses multiple ionizable functional groups. When the working medium is strongly acidic (pH below 3.5), it converts into a positively charged ion due to the protonation of the dimethyl ammonium group. When the pH of the working medium is between 3.5 and 7.5, it exists in the zwitter ionic form due to the loss of the phenolic functional group. When the pH of the working medium exceeds 7.5, it is present as a negatively charged ion due to the deprotonation of the tricarbonyl and phenolic groups (Filik et al 2016). Therefore, the peak potential and peak current of TC are dependent on the pH of the analyte solution. It has been observed that the peak current of TC increases with pH, reaching a maximum at pH 6.0. Consequently, this pH value was selected for the present study. Additionally, as the pH of the analyte solution increases, the peak potential of TC shifts toward more negative potential values.

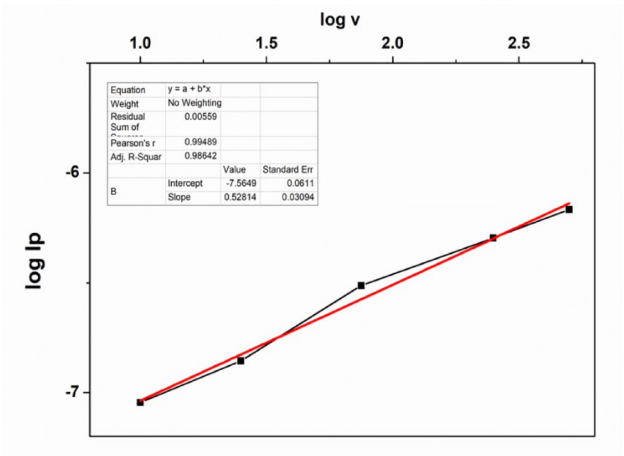

Fig. 4 log v-log Ip graph of electrochemical behavior of tetracycline on GA_2-Fe_2O_3/GCE electrode

Investigating the effect of scan rate on peak current

To investigate the electrochemical behavior of TC on GA_2-Fe_2O_3/GCE, the effect of scan rate on peak current was studied using the CV method. Scan rate voltamograms of 5.96×10^{-5} M TC in pH 6 BR buffer on GA_2-Fe_2O_3/GCE in the range of 5–1000 mVs^{-1} are shown in Fig. 4. When the logarithm of the scan rate (log υ) is plotted against the logarithm of the peak current (log Ip), the linear equation shown below is obtained:

$$\log Ip = 0.547 \log v \left(\text{mV s}^{-1}\right) - 7.626 \ R^2 = 0.979$$

Since the slope in this equation is 0.547, it is understood that the behavior of TC on GA_2-Fe_2O_3/GCE is diffusion-controlled (Laviron et al. 1980).

The $v^{1/2}$ vs. Ip graph derived from the voltammograms obtained by applying different scan rates in the 5¯1000 mVs^{-1} scan rate range of TC is shown in Fig. S6.

The obtained equation is given below.

$$Ip\,(A) = 1.2059x10^{-6} v^{1/2} \left(Vs^{-1}\right) - 4.75 \times 10^{-8} \left(R^2 = 0.990\right)$$

In this equation, it is seen that the square root of the scan rate and the peak current are linear.

The TC contains four aromatic rings (Fig. S1). The oxidation mechanism of TC was well defined by Sun et al. 2017. They stated that, in the TC structure, the hydroxyl group of the tenth carbon atom loses an electron and a proton, becoming an oxygen free radical. However, it is very unstable in solution and quickly loses another electron,forming a double oxygen bond. Then a portion of TC forms a tighter, positively charged structure that directly loses two electrons and a proton. It then combines with the strongly negatively

charged oxygen in hydrone, losing two electrons and three protons to form a new substance containing the quinone structure. In this study, the electrochemical analysis of TC in pH 6 BR buffer was investigated. TC underwent an oxidation reaction in a basic environment on a GA_2-Fe_2O_3/GCE working electrode. Two irreversible oxidation peaks were observed. For a completely irreversible system, Laviron's equation is as follows (Laviron 1979):

$$E_{p=}E^{0'} + \left(\frac{2,303RT}{\alpha nF}\right)\log\left(\frac{RTk^0}{\alpha nF}\right) + \left(\frac{2,303RT}{\alpha nF}\right)logv$$

Here:

- Ep: Peak potential (V).
- α: Electron transfer coefficient (usually assumed to be 0.5).
- n: Total number of electrons transferred.
- v: Scan rate (V s^{-1}).
- R, T, F: Gas constant (8.314), temperature (298 K) and Faraday constant (96,485 C/mol).

Theslope of lnv-Epa graph is given in the following equation as m:

$$m = \frac{2,303RT}{\alpha nF}$$

Accordingto O_2 oxidation peak of TC with a concentration of 5.96×10^{-5} M TC pH6 BR buffer in the potential range of 0 V to 1.5 V at scan rates of 10, 25, 50, 75, 100, 150, 250, 500, 750, 1000 mV s^{-1} the lnv-Epa graph was plotted (Fig. S7). The number of electrons lost in their reversible oxidation reaction (n) was calculated as 3,9 (n≈4).This result is consistent with Sun et al 2017.

Voltammetric determination of TC with GA_2-Fe_2O_3/GCE

Voltammetric determination of TC was performed and recorded using the standard method with DPV over GA_2-Fe_2O_3/GCE in pH 6 BR buffer solution (Yıldız et al. 2026). Calibration graphs were plotted using the obtained results. The voltammograms and calibration graph are shown in Figs. 5 and 6, respectively.

Two linear operating ranges (LR1 and LR2) for TC were observed. These operating ranges are as follows: 1.0×10^{-6}–2.0×10^{-5} M and 2.0×10^{-5}–9.9×10^{-5} M, respectively. The equations and regression coefficients for this calibration graph are as in equations below:

$$\mathrm{Ip\,(A)} = 0.050\mathrm{C}\ \left(\mathrm{mol}\ L^{-1}\right) + 1.066\times10^{-7}\mathrm{R}^2 = 0.91 \quad \text{(LR1)}$$

$$\mathrm{Ip\,(A)} = 0.012\mathrm{C}\ \left(\mathrm{mol}\ L^{-1}\right) + 8.16\times10^{-7}\mathrm{R}^2 = 0.98 \quad \text{(LR2)}$$

From the calibration graph of the TC generated on GA_2-Fe_2O_3/GCE using the DPV method, the LOD value was calculated from the formula 3 s/m, and the LOQ value from the formula 10 s/m. Here, m is the slope of the calibration graph. In the first operating interval (LR1), the s value was 7.97×10^{-9}. Ten repeated voltamograms of the 1.99×10^{-6} M TC were taken, and 5 closely related peak currents were

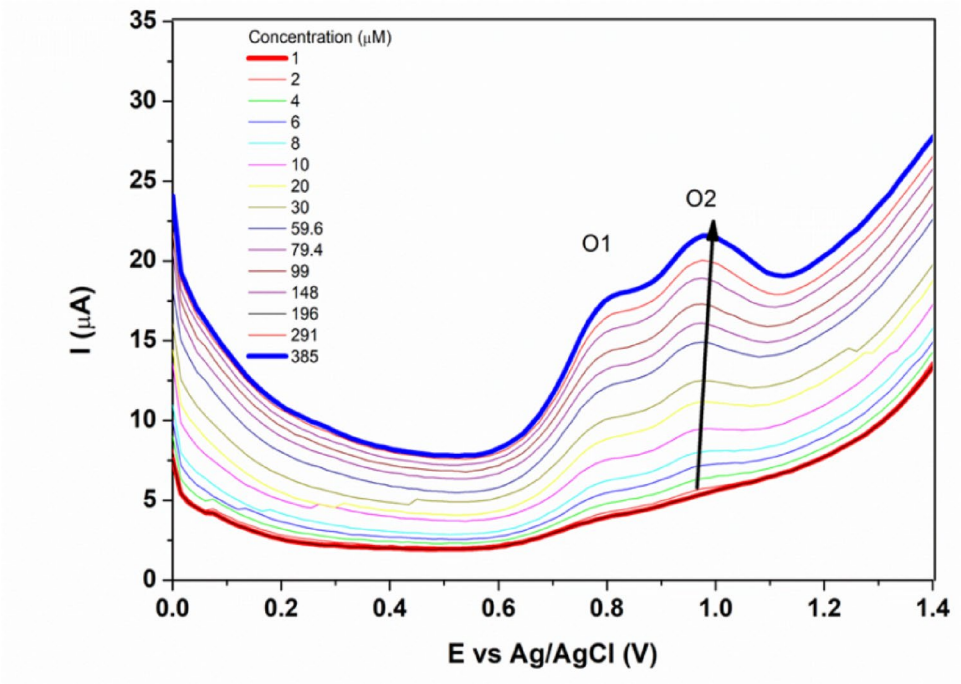

Fig. 5 DPV voltammograms of TC with different concentrations on GA_2-Fe_2O_3/GCE in pH 6 BR buffer

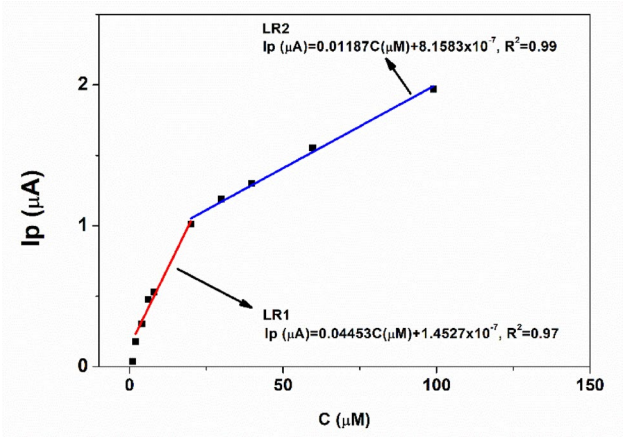

Fig. 6 Calibration line obtained from DPV voltammograms of TC with different concentrations on GA_2-Fe_2O_3/GCE in pH 6 BR buffer

identified from these, and the standard deviation of the peak current was calculated, resulting in an s value of 7.97×10^{-9}. The corresponding LOD and LOQ values for first linear working ranges were as follows: 4.78×10^{-7} M; 1.59×10^{-6} M, respectively. For the second linear working range, ten repeated voltamograms of the 2.0×10^{-5} M TC were taken, and 5 closely related peak currents were identified from these, and the standard deviation of the peak current was calculated, resulting in an s value of 4.98×10^{-8}. The corresponding LOD and LOQ values for the first linear working ranges were as follows: 2.13×10^{-5} M; 7.11×10^{-5} M, respectively.

The results obtained show that TC can be determined on GA_2-Fe_2O_3/GCE at low concentrations over a wide working range of 1.0×10^{-6}–9.9×10^{-5} M.

In addition, the intraday repeatabilities of the peak currents and peak potentials measured on the GA_2-Fe_2O_3/GCE surface with 1.99×10^{-6} M, 2.0×10^{-5} M, and 7.9×10^{-5} M TC were investigated. The intraday repeatabilities (RSD%) of the peak current of 1.99×10^{-6} M, 2.0×10^{-5} M, and 7.9×10^{-5} M TC were calculated as 3.32, 5.90, and 5.62, respectively. No deviation was observed in the peak potential. The fact that the RSD% values are about 5% indicates that the repeatability is good for this electrode.

To investigate the reproducibility of GA_2-Fe_2O_3/GCE, 5 different modified electrodes were prepared under the same composition and conditions. The electrode was examined using the DPV method in pH 6 BR buffer containing 1.99×10^{-6} M TC. The reproducibility (RSD%) of the inter-day peak current and peak potential of the modified electrode was as follows: 3.72 and 0.73, respectively. For this electrode, the RSD% of the peak current and potential values was obtained below 5%. Based on these results, it can be said that the reproducibility of the GA_2-Fe_2O_3/GCE electrode is good.

A comparative study of TC determination with different electrodes

Table 3 provides a comparison of the developed method for determining TC using the DPV method with GA_2-Fe_2O_3/GCE electrodes with some previous methods in the literature.

The results in Table 3 clearly show that the retention method has a lower LOD structure compared to Turbale et al. 2020. Furthermore, LOD results close to those of Huong et al. 2023 were obtained. The advantage of this effective modification electrode usage is that TC analysis does not require an electrode surface cleaning pretreatment.

Pharmaceutical analysis

In the preparation of tablet samples, 250 mg tablets of Tetra® Gensenta tablets were used. Ten tablets were weighed individually, and the average mass of one tablet was determined as 0.3615 g. All of these weighed tablets were ground into powder using a porcelain mortar. The powdered tablets were weighed to a concentration of 1.0×10^{-2} M and diluted with ethanol to a volume of 50 mL. Before use, these prepared samples were kept in an ultrasonic bath for 30 min and then filtered through filter paper. This prepared solution was used as the analyte in the tablet studies. In addition, voltamograms were obtained by adding a standard from the TC tablet solution to a pH 6 BR buffer solution using the DPV method on GA_2-Fe_2O_3/GCE. Using this, a calibration curve was drawn, and two operating ranges for the TC tablet solution were observed. These are 1.0×10^{-6}–10×10^{-6} M and 1.0×10^{-5}–14.8×10^{-5} M, respectively. Their calibration graph is shown in Fig. 7.

The equations and regression coefficients for this calibration graph are as follows.

$$\mathrm{Ip\,(A)} = 0.073\ \mathrm{C}\ \left(\mathrm{mol}\ L^{-1}\right) + 2.87 \times 10^{-7}\mathrm{R}^2 = 0.99 \quad \text{(LR1)}$$

$$\mathrm{Ip\,(A)} = 0.0072\ \mathrm{C}\ \left(\mathrm{mol}\ L^{-1}\right) + 9.85 \times 10^{-7}\mathrm{R}^2 = 0.99 \quad \text{(LR2)}$$

The LOD value was calculated from the calibration graph of the TC inside the tablet, generated by the DPV method on GA_2-Fe_2O_3/GCE, using the formula 3 s/m, and the LOQ value was calculated using the formula 10 s/m, where m is the slope of the calibration graph. Ten repeated voltamograms of the TC inside the tablet were taken during the first operating interval, and six closely spaced peak currents were identified. The standard deviation of the peak current was calculated, and the s value was found to be 1.26×10^{-8}. The corresponding LOD and LOQ values are: 5.21×10^{-7} M and 1.74×10^{-6} M, respectively. In the second operating interval, the s value was 1.99×10^{-5} M. Ten repeated voltamograms

Table 3 Comparative study of reported methods of TC determination with different electrodes

Electrodes	Detection method	Working environment	Linear range (mol L^{-1})	Limit of detection (mol L^{-1})	Referans
Glassy carbon electrode modified with poly(malachite green)	Square wave adsorptive anodic stripping voltammograms (SWAdASVs)	pH 7.5 PBS	50×10^{-6}–1.0×10^{-4}	1.6×10^{-6}	(Turbale et al. 2020)
Activated GCE	DPV	0.2 M Na_2SO_4 PH 2.5	2.0×10^{-6}–1.6×10^{-5} 1.6×10^{-5}–8.3×10^{-5}	2.3×10^{-7}	(Huong, et al. 2023)
Multi-Wall Carbon Nanotube–Ionic Liquid Film Coated Glassy Carbon Electrode	DPV	pH 7.0 PBS	1.1×10^{-7}–2.2×10^{-5}	3.0×10^{-8}	(Guo et al. 2009)
Graphene oxide-based UiO-66-NH_2 metal organic framework composite (GO/UiO-66-NH_2)/GCE	DPV	pH 2, PBS	4.5×10^{-9}–2.25×10^{-7} 2.25×10^{-7}–9.0×10^{-6}	6.75×10^{-9}	(Bigdelifam and Hashemi 2025)
GA_2-Fe_2O_3/GCE	DPV	pH 6, BR	1.0×10^{-6}–2.0×10^{-5} 2.0×10^{-5}–9.9×10^{-5}	4.78×10^{-7}	This work

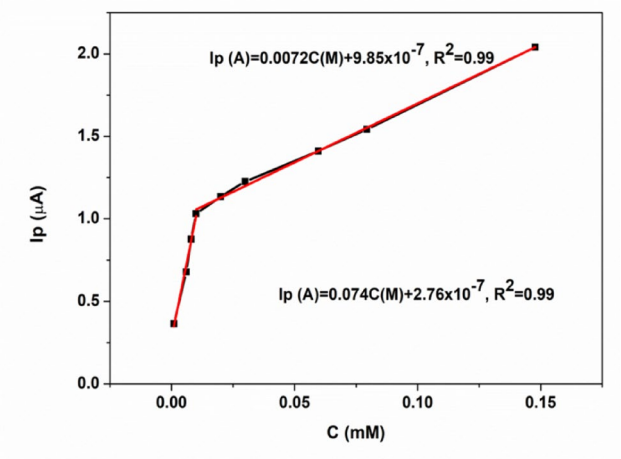

Fig. 7 Calibration line obtained from DPV voltammograms of TC in tablette sample with different concentrations on GA_2-Fe_2O_3/GCE in pH 6 BR buffer

of the TC inside the tablet were taken, and six closely spaced peak currents were identified. The standard deviation of the peak current was calculated, and the s value was found to be 1.21×10^{-8}. Their LOD and LOQ values are as follows: 5.0×10^{-6} and 1.7×10^{-5} M, respectively. In tablet recovery studies, recovery% values were calculated using the correct equations of the calibration graphs belonging to TC and are given in Table 4.

Assessment of the developed whiteness assessment

The sustainability and analytical efficiency of the proposed GA_2-Fe_2O_3/GCE/DPV method were quantitatively evaluated using the RGB 12 algorithm. Conducted within the framework of the White Analytical Chemistry (WAC) concept, this analysis simultaneously normalizes the method's analytical performance (Red), environmental sustainability (Green), and operational productivity (Blue)(Nowak et al 2021).

Table 4 Analysis results of GA_2-Fe_2O_3/GCE using the DPV method for Tetra® gensenta tablets containing TC in pH 6 BR buffer

Matter amount in label (mg)	50
Experimental matter content (mg)	0.971
Real matter content (mg)	0.962
*Mean Recovery%	100.94
Relative Error%	−0.94

* Analysis data was evaluated as 3 repetitions

Upon examination of the data presented in Table S1, it is observed that the developed sensor demonstrates performance exceeding the 90% threshold across all three primary parameters. The method's rapid response time of 30 s and minimal reagent consumption per analysis (at the microliter level) ensured the maximization of both "Blue" and "Green" scores. This multidimensional assessment academically validates that our modified electrode system not only offers high sensitivity and selectivity but also constitutes a sustainable, cost-effective alternative for routine laboratory applications in strict adherence to modern green chemistry principles.

Conclusions

In this study, GA_2-Fe_2O_3/GCE) was used as a sensor for the electrochemical analysis of TC in drug formulations. After optimizing the experimental conditions, the effects of pH and scan rate on the peak current were investigated. The highest peak current was obtained at pH 6. The effect of scan rate on the peak current was determined to be diffusion-controlled behavior of the TC on the electrode surface. For the characterization of the electrode surface, cyclic voltamograms were recorded on GCE and GA_2-Fe_2O_3/GCE in 1 mM $K_3Fe(CN)_6$ and 0.1 M KCl solutions at different scan rates (5–1000 mV s^{-1}). Using these, the surface areas of GCE and GA_2-Fe_2O_3/GCE were calculated. Following these studies, the working range, (LOD), and LOQ of TC with GA_2-Fe_2O_3/GCE were found to be as follows: 1.0×10^{-6}–9.9×10^{-5} M; 4.78×10^{-7} M and 1.59×10^{-6} M, respectively. In addition, the working range, LOD, and LOQ values of the tablet for the applicability of the developed method were found to be as follows: 1.0×10^{-6}–14.8×10^{-5} M; 5.21×10^{-7} M and 1.74×10^{-6} M, respectively. The applicability of the method was demonstrated by recovery studies in the tablet, and the recovery rate in the tablet was calculated as 100.94%.

Supplementary Information The online version contains supplementary material available at https://doi.org/10.1007/s11696-026-05240-3.

Author contributions BK:Conceptualization, Methodology, Software, Validation, Formalanalysis, Investigation, Resources, Data Curation, Writing—OriginalDraft, Writing—Review& Editing, Visualization Yİ:Conceptualization, Methodology, Software, Validation, Formalanalysis, Investigation, Resources, Data Curation, Writing—OriginalDraft, Writing—Review& Editing, Visualization.

Funding Open access funding provided by the Scientific and Technological Research Council of Türkiye (TÜBİTAK).

Data availability No datasets were generated or analysed during the current study.

Declarations

Conflict of interest The authors declare no Conflict of interest.

Open Access This article is licensed under a Creative Commons Attribution 4.0 International License, which permits use, sharing, adaptation, distribution and reproduction in any medium or format, as long as you give appropriate credit to the original author(s) and the source, provide a link to the Creative Commons licence, and indicate if changes were made. The images or other third party material in this article are included in the article's Creative Commons licence, unless indicated otherwise in a credit line to the material. If material is not included in the article's Creative Commons licence and your intended use is not permitted by statutory regulation or exceeds the permitted use, you will need to obtain permission directly from the copyright holder. To view a copy of this licence, visit http://creativecommons.org/licenses/by/4.0/.

References

Abood ES, Abed AS, Salman ZN (2021) New Fe_2O_3 nanoparticles modified carbon paste electrode: a cyclic voltammetric study. Egypt J Chem 64(12):7509–7515. https://doi.org/10.21608/EJCHEM.2021.100563.4672

Adabi M, Reza Faryabi M, Nili-Ahmadabadi A, Gharekhani J, Mehri F (2024) Evaluation of tetracycline antibiotics residues in chicken tissues using the four-plate test, ELISA, and HPLC methods in Iran. J Environ Anal Chem 104(9):2014–2023. https://doi.org/10.1080/03067319.2022.2054710

Allahverdiyeva S, Yardım Y, Şentürk Z (2021) Electrooxidation of tetracycline antibiotic demeclocycline at unmodified boron-doped diamond electrode and its enhancement determination in surfactant-containing media. Talanta 223:121695. https://doi.org/10.1016/j.talanta.2020.121695

Bard A J, Faulkner L R, White H S (2022) Electrochemical methods : fundamentals and applications .Jonh Willey and Sons.

Bigdelifam D, Hashemi M (2025) Mechanochemical synthesis of graphene oxide/UiO-66-NH2 nanocomposites: characterization and fabrication of an electrochemical sensor for the determination of tetracycline residues in milk samples. ACS Omega 10(16):16184–16193. https://doi.org/10.1021/acsomega.Ac09975

Burç M, Titretir Duran S, Güngör Ö, Karagözler AE (2024) Determination of gentamicin by using square wave anodic stripping voltammetry with poly (β-cyclodextrin-p-toluene sulfonic acid) modified glassy carbon electrode. Polym Bull 81(7):6381–6403. https://doi.org/10.1007/s00289-023-05011-0

Butovskaya E, et al (2024) Quantitative determination of tetracyclines in medicated feed for food-producing animals by HPLC–DAD. Food Addit Contam Part A Chem 41(6): 601–609. https://doi.org/10.1080/03067319.2022.2054710

Cánovas R, Sleegers N, van Nuijs AL, De Wael K (2021) Tetracycline antibiotics: Elucidating the electrochemical fingerprint and oxidation pathway. Chemosensors 9(7):187. https://doi.org/10.3390/chemosensors9070187

Chang D, Mao Y, Qiu W, Wu Y, Cai B (2023) The source and distribution of tetracycline antibiotics in China: a review. Toxics 11(3):214. https://doi.org/10.3390/toxics11030214

Chen X, Xu J, Li Y, Huang Y, Zhang L, Bi N, Jia L (2024) Recent progress in lanthanide-based fluorescent nanomaterials for tetracycline detection and removal. Microchim Acta 191(9):531. https://doi.org/10.1007/s00604-024-06607-7

Dinber B, Hilawea KT, Yihune E, Chanie G, Metto M, Bitew M, Getinet TT, Abebe A (2024) New Brønsted-Lowry acid Co (II) complexes: synthesis, characterization, and investigation of electrochemical application for sensing of salbutamol. Polyhedron 264:117248. https://doi.org/10.1016/j.poly.2024.117248

Đurović A, Stojanović Z, Bytešníková Z, Kravić S, Švec P, Přibyl J, Richtera L (2022) Reduced graphene oxide/ZnO nanocomposite modified electrode for the detection of tetracycline. J Mater Sci 57(9):5533–5551

Filik H, Avan A, Aydar A, Ozyurt S, Demirata B (2016) Determination of tetracycline on the surface of a high-performance graphene modified screen-printed carbon electrode in milk and honey samples. Curr Nanosci 12(4):527–533. https://doi.org/10.2174/1573413712666151214222808

Gab-Allah MA, Lijalem YG, Yu H, Lim DK, Ahn S, Choi K, Kim B (2023) Accurate determination of four tetracycline residues in chicken meat by isotope dilution-liquid chromatography/tandem mass spectrometry. J Chromatogr A 1691:463818. https://doi.org/10.1016/j.chroma.2023.463818

Gao F, Zhao Y, Dai X, Xu W, Zhan F, Liu Y, Wang Q (2024) Aptamer tuned nanozyme activity of nickel-metal–organic framework for sensitive electrochemical aptasensing of tetracycline residue.

Food Chem 430:137041. https://doi.org/10.1016/j.foodchem.2023.137041

Gholivand MB, Khani H (2013). Determination of tetracycline at a UV-ırradiated DNA film modified glassy carbon electrode. Electroanalysis, 25(2):461–467 https://doi.org/10.1002/elan.201200300

Guo G, Zhao F, Xiao F, Zeng B (2009) Voltammetric determination of tetracycline by using multi-wall carbon nanotube–ionic liquid film coated glassy carbon electrode. Int J Electrochem Sci 4(9):1365–1372. https://doi.org/10.1016/S1452-3981(23)15229-1

Guo W, Hu Y, Zhang X, Wang Y, Li Y, Wang Y (2024) Electrochemical determination of tetracycline using the synergy of a molybdenum (IV) sulfide-thionine nanocomposite with an aptamer by differential pulse voltammetry (DPV). Anal Lett 57(14):2364–2375. https://doi.org/10.1080/00032719.2023.2294355

Gupta A, Zgueb R, Korte D (2026) Characterisation of TiO_2-and Fe_2O_3-based nanocomposites by photothermal techniques for potential application as photocatalysts for water purification purposes. Photonics 13(4):313. https://doi.org/10.3390/photonics13040313

Harraz FA, Ismail AA, Al-Sayari SA, Al-Hajry A, Al-Assiri MS (2016) Highly sensitive amperometric hydrazine sensor based on novel α-Fe_2O_3/crosslinked polyaniline nanocomposite modified glassy carbon electrode. Sens Actuators B Chem 234:573–582. https://doi.org/10.1016/j.snb.2016.05.021

Hu F, Fu Q, Li Y, Yan C, Xiao D, Ju P, Ai S (2024) Zinc-doped carbon quantum dots-based ratiometric fluorescence probe for rapid, specific, and visual determination of tetracycline hydrochloride. Food Chem 431:137097. https://doi.org/10.1016/j.foodchem.2023.137097

Huong NT, Hien NTM, Thuy TTD, Ai NTN, Anh LDQ (2023) Determination of tetracycline residue in pork by differential pulse voltammetry using activated glassy carbon electrode. Vietnam J Chem 61(1):65–73. https://doi.org/10.1002/vjch.202200010

Ipek Y (2020) Electrochemical behaviour of cross-linker glutaraldehyde as a receptor for carbaryl biosensor. J Indıan Chem Soc 97(11 A): 2218–2223.

Iqbal Y, Ma W, Li X, Fu S, Shahzad A, Ahmad I, Abohashrh M (2025) A brief outlook on the preparation and magnetic properties of iron oxide nanoparticles for water remediation. Water Air Soil Pollut 236(11):687. https://doi.org/10.1007/s11270-025-8364-6

Keçeci A, Koçak B, İpek Y (2025) Highly sensitive DNA-based electrochemical biosensor for analysis of oseltamivir used in treatment of COVID–19. J Appl Electrochem 55(4):1073–1087. https://doi.org/10.1007/s10800-024-02213-w

Koçak B (2023) A selective and sensitive electrochemical sensor for pyridoxine hydrochloride (vitamin B6) in pharmaceutic tablet. ChemistrySelect 8(39):e202303112

Koçak B, İpek Y (2022) Electrochemical detection of ivermectin used for the treatment of COVID-19 with glutardialdehyde-modified glassy carbon electrode. Electrocatalysis 13(2):108–115. https://doi.org/10.1007/s12678-021-00704-4

Koçak B, İpek Y, Keçeci A (2023) A novel electrochemical sensor for metoprolol analysis based on glutardialdehyde–zinc oxide modified boron doped diamond electrode. Diam Relat Mater 131:109558. https://doi.org/10.1016/j.diamond.2022.109558

Laviron E (1979) Theuse of linear potential sweep voltammetry and of ac voltammetry for the study of the surface electrochemical reaction of strongly adsorbed systems and of redox modified electrodes. J Electroanal Chem Interfacial Electrochem 100(1–2):263–270

Laviron E, Roullier L, Degrand CJ (1980). A multilayer model for the study of space distributed redox modified electrodes: Part II. Theory and application of linear potential sweep voltammetry for a simple reaction. J Electroanal Chemistry 112:11

Luo Y, Shao F, Sun Y, Wang H, He Y, Wang Y, Xu D (2025) Synthesis of SnC@ Au@ Apta by electrospinning as an electrochemical sensor for detection of tetracycline. Talanta 281:126866. https://doi.org/10.1016/j.talanta.2024.126866

Luo Y, Shao F, Sun Y, Wang H, He Y, Wang Y, Xu D (2025) Synthesis of SnC@ Au@ Apta by electrospinning as an electrochemical sensor for detection of tetracycline.https://doi.org/10.1016/j.talanta.2024.126866

Magar HS, Hassan RYA, Mulchandani A (2021) Electrochemical impedance spectroscopy (EIS): principles, construction, andbiosensing applications. Sensors 21(19):6578. https://doi.org/10.3390/s21196578

Meklati FR, Panara A, Hadef A, Meribai A, Ben-Mahdi MH Dasenaki, ME, Thomaidis NS (2022) Comparative assessment of antibiotic residues using liquid chromatography coupled with tandem mass spectrometry (LC-MS/MS) and a rapid screening test in raw milk collected from the North-Central Algerian dairies. Toxics 10(1):19. https://doi.org/10.3390/toxics10010019

Metto M, Tesfaye A, Atlabachew M, Abebe A (2024) Selective and sensitive electroanalytical biosensor based on Poly ([Cu (H2O) 2P2] I2)/GCE for the determination of esomeprazole in pharmaceutical formulations and biological fluid samples. Int J Electrochem Sci 19(11):100837. https://doi.org/10.1016/j.ijoes.2024.100837

Metto M, Tesfaye A, Atlabachew M, Munshea A, Abebe A (2025) Sensitive and selective electrochemical biosensor based on Manganese (II) complex for simultaneous determination of adenine and guanine from clinical samples and DNA extract samples. Biosens Bioelectron X 24:100603. https://doi.org/10.1016/j.biosx.2025.100603

Nekoueian K, Kontturi KS, Meinander K, Quliyeva U, Kousar A, Durairaj V, Laurila T (2024) Advanced nanocellulose-based electrochemical sensor for tetracycline monitoring. Electrochim Acta 500:144639. https://doi.org/10.1016/j.electacta.2024.144639

Nowak PM, Wietecha-Posłuszny R, Pawliszyn J (2021) White analytical chemistry: an approach to reconcile the principles of green analytical chemistry and functionality. TrAC Trends Anal Chem 138:116223. https://doi.org/10.1016/j.trac.2021.116223

Sato N, Ohta Y, Haruta M, Takehara H, Tashiro H, Sasagawam K, Ohta J (2023) Electrochemical activities of Fe_2O_3-modified microelectrode for dopamine detection using fast-scan cyclic voltammetry. AIP Adv 13(2). https://doi.org/10.1063/5.0123865

Sun XM, Ji Z, Xiong MX, Chen W (2017) The electro chemical sensor for the determination of tetracycline based on graphene/l-cysteinecomposite film. J Electrochem Soc 164(4):B107–B112. https://doi.org/10.1149/2.0831704jes

Sun Y, Luo Y, Wang H, He Y, Wang R, Lu M, Xu D (2025) Electrochemical detection of tetracycline by zinc oxide modified with molecularly-imprinted polymers. Anal Methods 17(15):3027–3035. https://doi.org/10.1039/D5AY00270B

Tasci F, Canbay HS, Doganturk M (2021) Determination of antibiotics and their metabolites in milk by liquid chromatography-tandem mass spectrometry method. Food Control 127:108147. https://doi.org/10.1016/j.foodcont.2021.108147

Turbale M, Moges A, Dawit M, Amare M (2020) Adsorptive stripping voltammetric determination of Tetracycline in pharmaceutical capsule formulation using Poly (Malachite green) modified glassy carbon electrode. Heliyon 6(12). https://doi.org/10.1016/j.heliyon.2020.e05782

Urapen R, Masawat P (2015) Novel method for the determination of tetracycline antibiotics in bovine milk based on digital-image-based colorimetry. Int Dairy J 44:1–5. https://doi.org/10.1016/j.idairyj.2014.12.002

Vinay MM, Nayaka YA (2019) Iron oxide (Fe_2O_3) nanoparticles modified carbon paste electrode as an advanced material for electrochemical investigation of paracetamol and dopamine. J Sci Adv Mater Devices 4(3):442–450. https://doi.org/10.1016/j.jsamd.2019.07.006

Wang X, Li J, Jian D, Zhang Y, Shan Y, Wang S, Liu F (2021) based antibiotic sensor (PAS) relying on colorimetric indirect competitive enzyme-linked immunosorbent assay for quantitative tetracycline and chloramphenicol detection. Sens Actuators, B Chem 329:129173. https://doi.org/10.1016/j.snb.2020.129173

Wang L, Hu J, Wei W, Song Y, Li Y, Shen Y, Qin L (2024) Electrochemical paper-based sensor based on molecular imprinted polymer and nitrogen-doped graphene for tetracycline determination. Microchem J 207:111809. https://doi.org/10.1016/j.microc.2024.111809

Yıldız C, Pekin Turan M, Eskiköy Bayraktepe D, Yazan Z (2026) A magnetite-cerium oxide nanocomposite-based electrochemical dna biosensor for highly sensitive detection of 4-nonylphenol in food samples. Electroanal 38(1):e70102. https://doi.org/10.1002/elan.70102

Zhang L, Yin M, Wei X, Sun Y, Luo Y, Lin H, Xu D (2024a) An aptamerelectrochemical sensor based on functional carbon nanofibers for tetracycline determination. Bioelectrochemistry 157:108668. https://doi.org/10.1016/j.bioelechem.2024.108668

Zhang M, Zhang S, Xu Z, Lv T, Liu X, Wang L, Liu B (2024b) Fluorescence determination of the total amount of tetracyclines by a flavonol-based supramolecular sensor. Talanta 266:124982. https://doi.org/10.1016/j.talanta.2023.124982

Zhao L, Wang T, Jiang S, Liu T, Lu Z Su G, Song C (2024) Hollow CoZnSe@ CN nanocage with enzymatic activity for determination of tetracycline using smartphone platforms and virtual reality revealing. Microchim Acta 191(1):79.

Zhou T, Halder A, Sun Y (2018) Fluorescent nanosensor based on molecularly imprinted polymers coated on graphene quantum dots for fast detection of antibiotics. Biosens 8(3):82. https://doi.org/10.3390/bios8030082

Publisher's Note Springer Nature remains neutral with regard to jurisdictional claims in published maps and institutional affiliations.

Authors and Affiliations

Berna Koçak[1] · Yeliz İpek[1]

✉ Berna Koçak
bernakocak@munzur.edu.tr

Yeliz İpek
yelizipek@munzur.edu.tr

[1] Chemistry and Chemical Process Technologies Department, Vocational School of Tunceli, Munzur University, 62000 Tunceli, Turkey